80-12

School of

OCEANOGRAPHY

Interrelationships Between Optical Parameters, Biological Parameters and Particle Size Distributions in Monterey Bay

by
James C. Kitchen
and
J. Ronald V. Zaneveld

National Aeronautics and Space Administration
Contract NAS5-23738

Reference 80-12
June 1980
Final Report

OREGON STATE UNIVERSITY

INTERRELATIONSHIPS BETWEEN OPTICAL PARAMETERS, BIOLOGICAL PARAMETERS AND PARTICLE SIZE DISTRIBUTIONS IN MONTEREY BAY

Final Report

Contract NAS5-23738

Submitted to

National Aeronautics and Space Administration

by

James C. Kitchen and J. Ronald V. Zaneveld

School of Oceanography
Oregon State University
Corvallis, Oregon 97331

Reference 80-12
June 1980

G. Ross Heath
Dean

ABSTRACT

Spectral beam attenuation coefficients, spectral volume scattering function meaurements at 45°, 90°, and 130°, particle size distributions and chlorophyll a and phaeophytin pigment concentrations were measured during May and September, 1977 in Monterey Bay, California. This data is examined and statistical interrelationships between the parameters measured are explored.

It was found that beam attenuation and suspended particulate volume concentration are highly correlated with the slope of the particle size distribution, low slopes corresponding to higher particle concentrations. Correspondingly, the slope of the spectrum of the particulate beam attenuation decreases with increasing particle concentration. This decrease is not as much as theoretical values based on hyperbolic size distributions extending to zero particle size would predict, but such theoretical values are based on diameters which we cannot measure nor do we expect the hyperbolic distribution to hold to such small sizes. Changes in the type of particles present with changing particle concentration also affect the spectral properties.

Variations in the spectral behavior with location both horizontally and vertically were found. These variations were partially explained by corresponding changes in particle size distributions and biological parameters. The volume scattering functions behaved similarly to the beam attenuation coefficients except that the particle size distributions were not able to explain much additional variation in the scattering beyond that explained by total attenuation and location parameters. Unmeasured parameters such as particle shape may be more important for scattering than attenuation in explaining spectral and angular differences between locations.

The particle size distributions and especially the larger particles were more important than the pigment parameters in predicting certain ratios of particulate spectral beam attenuation coefficients such as $C_p(450)/C_p(500)$, $C_p(400)/C_p(650)$ and $C_p450/C_p(650)$. The ratio of pigments to suspended volume was also significant in determining these ratios, and is believed to be related to the effective index of refraction for the collection of suspended particles. An exception was the parameter $C_p(400)/C_p(450)$ which was not predicted well by the slope of the size distribution. Instead, the pigment-suspended volume ratio and total suspended volume were foremost in importance followed by the concentration of the smallest measured particles (1.75-2.5 μm diameter) and the ratio of the small particles to medium-sized particles (6.2-10 μm). This particle ratio may extrapolate to the very small size particles better than the overall slope and thus be related to Rayleigh (λ^{-4}) scattering which might affect $C_p(400)/C_p(450)$ while the large particle scattering dominates the other ratios.

Particle size distributions were best predicted by the sum of the attenuation values and $C_p(400)/C_p(650)$. While several other parameters removed a statistically significant amount of additional variance, they did not improve the models for practical purposes. Particles less than 10 μm diameter had much smaller original variance (on a logarithmic scale) than the larger particles and not much variance was removed by the attenuation parameters. Better correlations would have resulted if an electronically tripped rosette sampler had been attached to the transmissometer package instead of relying on separate bottle costs.

The findings of this report were not even consistent between May and September and therefore it is highly unlikely that they could be applied

to other regions. A better approach would be to confine the area of interest both vertically and geographically, determine typical particle collections on which to do laboratory experiments and then use matrix minimization techniques to decompose measured optical spectra into the predetermined possible components.

TABLE OF CONTENTS

LIST OF FIGURES

LIST OF TABLES

LIST OF SYMBOLS

$a(\lambda)$ the light absorption coefficient (m^{-1}) at wavelength λ

$a_y(\lambda)$ the light absorption coefficient (m^{-1}) of dissolved organic substances found in seawater commonly referred to as "yellow matter."

$B(\theta,\lambda)$ the volume scattering function (m^{-1} $steradian^{-1}$) at an angle θ from the main light beam for light of wavelength λ.

$B_p(\theta,\lambda)$ the part of the volume scattering function, B, (m^{-1} $steradian^{-1}$) due to suspended particles.

BT the sum of the volume scattering functions, B, at angles of 45°, 90°, and 135° and at wavelengths of 400, 450, 500 and 550°.

BT1 = BT if the sample is from less than 40 m depth in water deeper than 40 m; otherwise BT1 = 0.

BT2 = BT if the sample is from more than 20 m depth in water between 20 and 40 m deep; otherwise BT2 = 0.

BT3 = BT if the sample is from 20 m or less depth in water between 20 and 40 m deep; otherwise BT3 = 0.

BT4 = BT if the sample is the one taken nearest bottom in less than 20 meters of water; otherwise BT4 = 0.

BT5 = BT if the sample is not the one taken nearest bottom and the water depth is less than 20 meters; otherwise BT5 = 0.

BTCR = BT if the sample was taken during the May cruise; = 0. if the sample was taken during the September cruise.

$B_w(\theta,\lambda)$ that portion of the volume scattering function, B, due only to optically pure water.

$c(\lambda)$ the beam attenuation coefficient (m^{-1}) for light of wavelength λ.

C particulate carbon concentration ($\mu g\ l^{-1}$).

CHL chlorophyll a concentration ($\mu g\ l^{-1}$).

CN the ratio of particulate carbon to particulate nitrogen.

$C_p(\lambda)$ that portion of the beam attenuation (m^{-1}) not due to optically pure water; "particulate attenuation."

$C_p'(\lambda)$ the particulate attenuation of wavelength λ divided by the sum of the particulate attenuations at 400, 450, 500, 550, 600 and 650 nm wavelength.

C_pT the sum of the particulate attenuation at 400, 450, 500, 550, 600 and 650 nm wavelength.

CR = 1. if the sample was taken during the May cruise and CR = 0. if the sample was taken during the September cruise.

CT1 = C_pT if G1 = 1. otherwise CT1 = 0.

CT2 = C_pT if G2 = 1. otherwise CT2 = 0.

CT3 = C_pT if G3 = 1. otherwise CT3 = 0.

CT4 = C_pT if G4 = 1. otherwise CT4 = 0.

CT5 = C_pT if G5 = 1. otherwise CT5 = 0.

CTCR = C_pT if CR = 1. otherwise CTCR = 0.

$C_w(\lambda)$ that portion of the beam attenuation, c, (m^{-1}) due to optically pure water.

F a statistical test value which for the stepwise regressions is equal to the mean reduction sum of squares divided by the mean residual sum of square errors.

G1 = 1.0 if the sample was taken from less than 40 m depth in water deeper than 40 m, otherwise G1 = 0.

G2 = 1.0 if the sample was taken from greater than 20 m depth in water between 20 and 40 m deep, otherwise G2 = 0.

G3 = 1.0 if the sample was taken from 20 m depth or less in water between 20 and 40 m deep; otherwise G3 = 0.

G4 = 1.0 if the sample was the one taken nearest bottom in water less than 20 m deep; otherwise G4 = 0.

G5 = 1.0 if the sample was not the one taken nearest bottom and the water was less than 20 m deep; otherwise G5 = 0.

LP0 the natural logarithm of P0

LP1 the natural logarithm of P1

LP2 the natural logarithm of P2

LP3 the natural logarithm of P3

LP4 the natural logarithm of P4

LP5 the natural logarithm of P5

LP6 the natural logarithm of P6

LVOL	the natural logarithm of VOL
m	a degree-of-freedom parameter for the greatest characteristic root test. In Table VI it is the index of refraction of a particle relative to water.
n	a degree-of-freedom parameter for the greatest characteristic root test.
N	particulate nitrogen concentration ($\mu g\ l^{-1}$)
ORG	the sum of the chlorophyll *a* and phaeophytin concentrations ($\mu g\ l^{-1}$).
p	the probabiliy that a statistical null-hypothesis is true. For example, that a regression coefficient is 0.
P0	the number of particles in one ml of sample with spherical equivalent diameters between 1.75 and 2.5 μm.
P1	the number of particles in one ml of sample with spherical equivalent diameters between 2.5 and 4.0 μm.
P2	the number of particles in one ml of sample with spherical equivalent diameters between 4.0 and 6.2 μm.
P3	the number of particles in one ml of sample with spherical equivalent diameters between 6.2 and 10 μm.
P4	the number of particles in one ml of sample with spherical equivalent diameters between 10 and 16 μm.
P5	the number of particles in one ml of sample with spherical equivalent diameters between 16 and 25 μm.
P6	the number of particles in one ml of sample with spherical equivalent diameters between 25 and 40 μm.
P1'	a transformation (as given on page 30) of P1 that first equalizes the variance with that of the other size classes and then removes concentration relative to other samples in favor of concentration relative to the other size classes for the same sample.
P2'	a transformation (as given on page 30) of P2 that first equalizes the variance with that of the other size classes and then removes concentration relative to other samples in favor of concentration relative to the other size classes for the same sample.

P3' a transformation (as given on page 30) of P3 that first equalizes the variance with that of the other size classes and then removes concentration relative to other samples in favor of concentration relative to the other size classes for the same sample.

P4' a transformation (as given on page 30) of P4 that first equalizes the variance with that of the other size classes and then removes concentration relative to the other samples in favor of concentration relative to the other size classes for the same sample.

P5' a transformation (as given on page 30) of P5 that first equalizes the variance with that of the other size classes and then removes concentration relative to other samples in favor of concentration relative to the other size classes for the same sample.

P6' a transformation (as given on page 30) of P6 that first equalizes the variance with that of the other size classes and then removes concentration relative to the other samples in favor of concentration relative to the other size classes for the same sample.

PCO the ratio of the sum of the chlorophyll a and phaeophytin concentrations to the suspended volume concentration ($\mu g\ \mu l^{-1}$)

PCU the ratio of the phaeophytin concentration to the sum of the phaeophytin and chlorophyll a concentrations.

PES P1/(P3 + P5)

PHE the phaeophytin concentration ($\mu g\ l^{-1}$)

PMM P2/P4

r the correlation coefficient, see r^2

r^2 the ratio of the reduction sum of squares to the original variance about the mean.

s a degree of freedom parameter for the greatest characteristic root test.

SH9 B(45,550)/B(90,550)

SH13 B(45,500)/B(135,500)

SLP the differential hyperbolic slope of the particle size distribution

SP4 B(45,400)/B(45,500)

SP9	B(90,400)/B(90,500)
SP13	B(135,400)/B(135,550)
SPE	Cp(400)/Cp(650)
SPEM	Cp(400)/CP(500)
SPES	CP(400)/(Cp(500) + Cp(650))
SPET	Cp(650)/CpT
SPM	Cp(450)/Cp(500)
SPME	Cp(450)/Cp(650)
SPSE	(Cp(400)/Cp(450)
t	a statistical test value equal to the ratio of a parameter to the standard deviation of that parameter.
Tr	the ratio of the intensity of a light beam after transversing a meter path to the intensity of the same beam before transversing the path, generally used in this text for light of 650 nm wavelength.
ν	the differential hyperbolic slope of the particle size distribution (Table VI).
λ	the wavelength of the light (nm); also the greatest characteristic root for testing multivariate analysis hypotheses.
θ	the angle away from the light beam; also $\lambda/(1+\lambda)$ in multivariate analysis.
σ	standard deviation from the mean value.

INTERRELATIONSHIPS BETWEEN OPTICAL PARAMETERS, BIOLOGICAL PARAMETERS AND PARTICLE SIZE DISTRIBUTIONS IN MONTEREY BAY

I. INTRODUCTION

During May and September 1977, cruises were taken in Monterey Bay to study the relationship of ocean color spectra and *in situ* optical, hyrographic and chemical parameters. The *in situ* data was published in (Zaneveld *et al.*, 1978). This report explores the relationships between these *in situ* parameters with two objects to accomplish: 1) to gain further understanding of the behavior of optical properties, and 2) to find algorithms for obtaining information about the particle size distribution from the easier to obtain optical data.

II. SPECTRAL BEAM ATTENUATION

Spectral beam attenuation values (C) were computed from measurements of light transmission (Tr) with an instrument described in (Zaneveld *et al.*, 1978). Six wavelengths were used with nominal values of 400, 450, 500, 550, 600 and 650 nm. Transmission being a ratio of power received to power output (corrected for lens interface effects) is a number less than 1.0. Attenuation is computed as follows: $C = - \ln (Tr)$. We are also interested in the attenuation due to elements (mainly particles) other than the water itself. This we will call particulate attenuation, Cp, although it may also be affected by dissolved substances ("yellow matter") which have highly variable concentrations in the ocean. $Cp = C - Cw$ where Cw is the attenuation due to pure seawater. All these parameters vary with wavelength and thus we have six values of Cp, C and Cw. We use the values of Cw given by Jerlov (1976) after Sullivan (1963) for pure water. Addition of sea salts to pure water causes no appreciable change in Cw in the spectral region in which we are interested (Jerlov, 1976).

Figure 1 shows the spectral characteristics of beam attenuation (C) and particulate beam attenuation (Cp) as a function of water clarity. Water clarity is here defined by the transmission of light at 650 nm wavelength. The samples were grouped in the intervals 1.5-5, 5-10, 10-15, 15-25, 25-35, 35-45, 45-55 and greater than 55% (55% = 0.55, a number less than one) transmission.

The beam attenuation displays the well known shift from a strong minimum in the blue to a broad minimum in the yellow-green region with increasing turbidity. Even in the most turbid water, however, light is attenuated more at 650 nm wavelength than in the region from 400-600 nm.

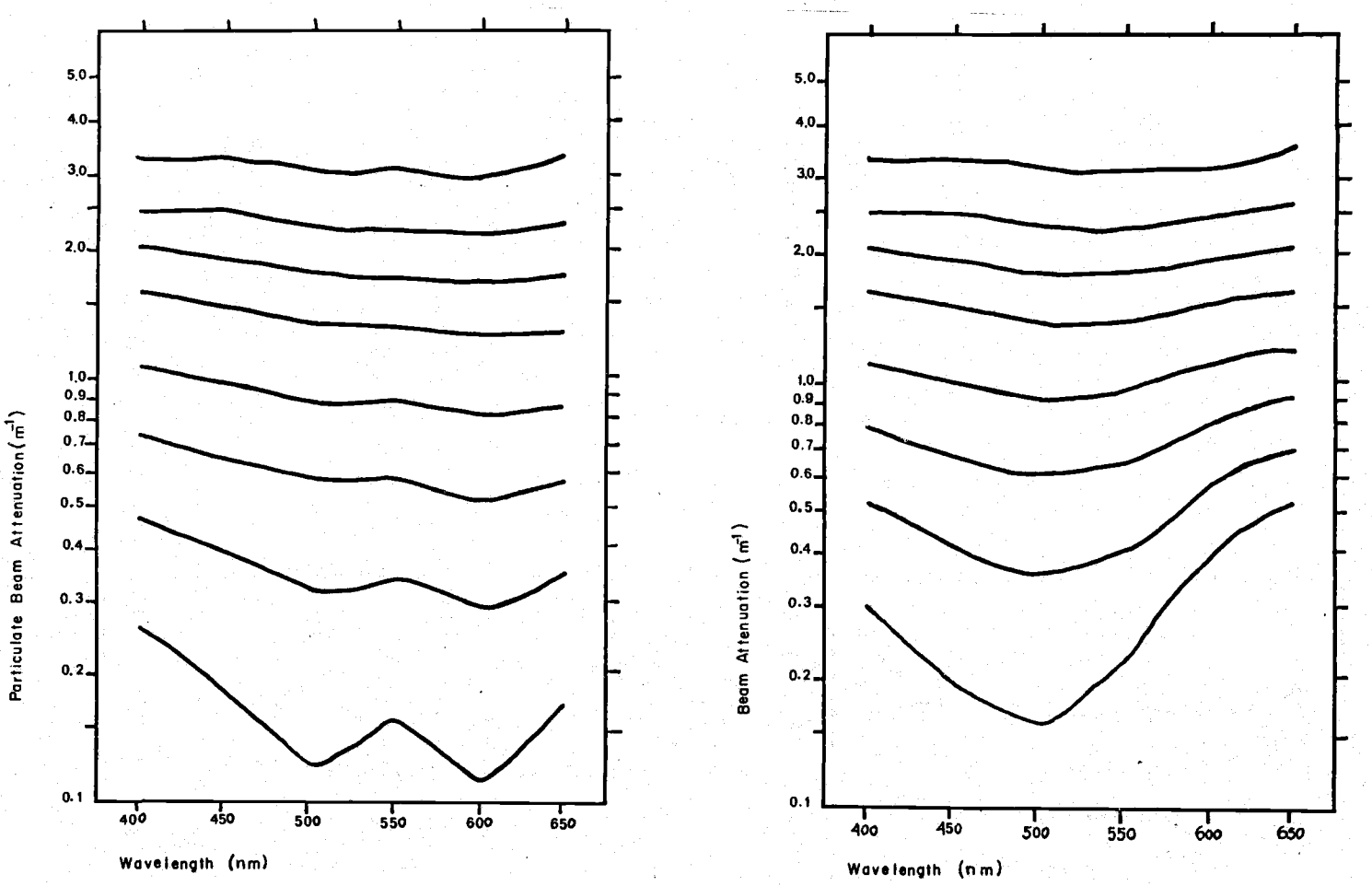

Figure 1. Average attenuation and particulate attenuation spectra for samples grouped according to their light transmission values at 650 nm wavelength (i.e., 1.5-5, 5-10, 10-15, 15-25, 25-35, 35-45, 45-55 and greater than 55% transmission).

The particulate attenuation is irregular in clear water, probably indicating an uncertainty of about 2% transmission (out of 80% measured transmission). Possible sources of this error are uncertainty in the values of the spectral attenuation of pure seawater, error in calibration, and perhaps a several nanometer wavelength shift from the nominal wavelength by the light-filter-detector system. This error rapidly decreases in importance with increasing turbidity. The most noticeable feature of the spectra is the decreasing slope of the curves with increasing attenuation. The ratio $C_p(400)/C_p(650)$ (an estimate of the slope of the spectrum) shows a monotonic decrease from 1.52 to 1.00 as the water becomes less transparent. If particulate attenuation was inversely proportional to wavelength, the value obtained for $C_p(400)/C_p(650)$ would be 1.625. Considering the uncertainties in the values of clean water, we could say that the general wavelength (λ) dependence of C_p is approximately as λ^{-1} for clean waters and decreases to no dependence (except in limited regions of wavelengths) for very turbid waters.

This variation may be explained in the following manner. As water becomes more turbid, it usually contains not only more particles, but a larger proportion of large particles as well. This is primarily a biological response to increased nutrient concentrations (Kitchen et al., 1975, 1978) and as such does not necessarily apply to bottom nepheloid layers. In Monterey Bay, however, the shelf was so shallow (~ 20 m) that no distinction can be made between surface waters and bottom waters. Thus, we get a good relationship (Figure 2) between water clarity and particle size distribution slope. Large values of slope indicate that the concentration of particles fall off rapidly with increasing particle size, thus indicating relatively more small particles. Small particles that have diameters close to the

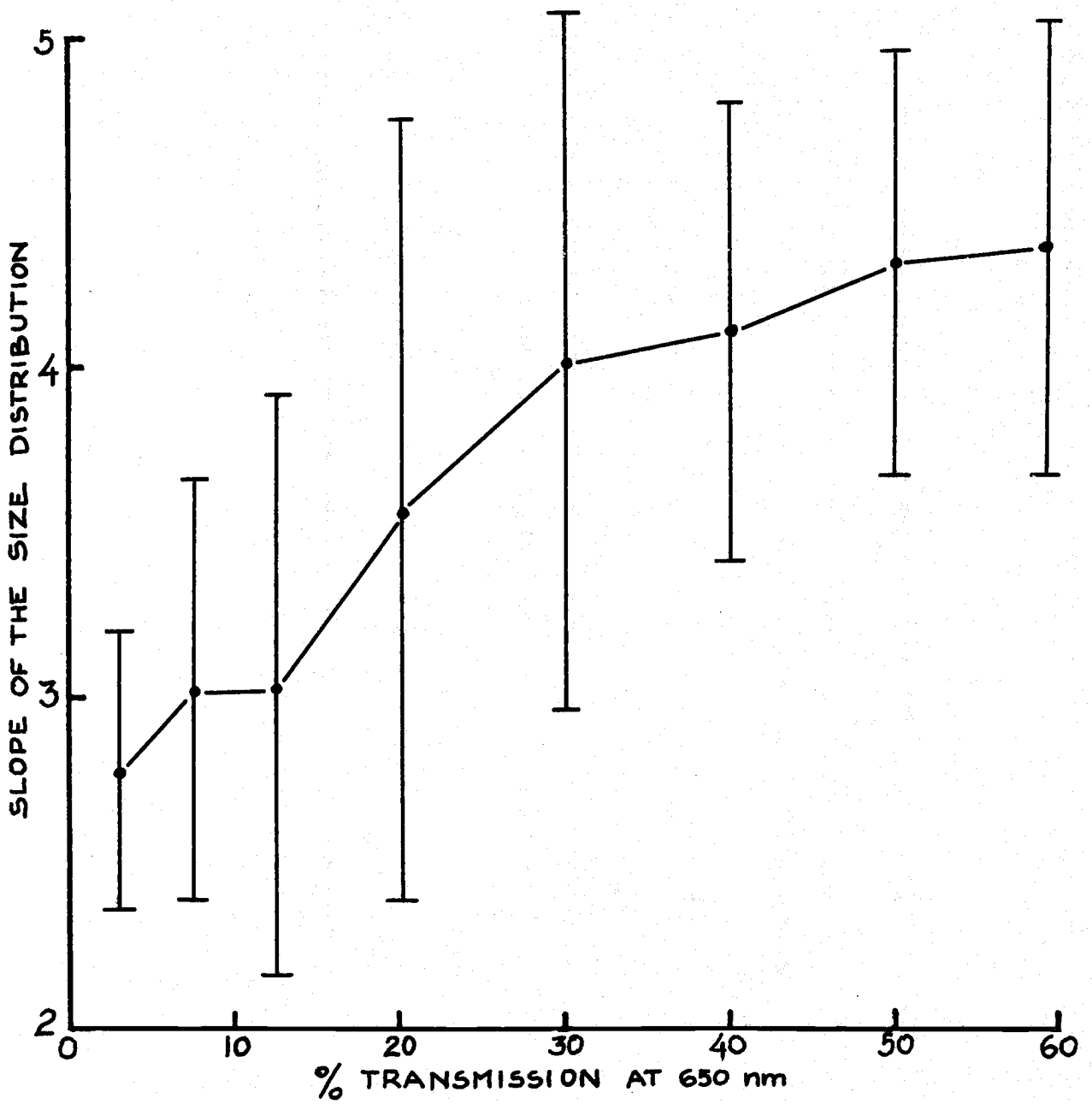

Figure 2. Relationship between slope of the particle size distributions and light transmission at 650 nm. Bars are 95% confidence limits for the population of samples within given transmission group.

wavelength of light are highly ($\sim \lambda^{-1}$) wavelength selective (Morel, 1973) while particles more than an order of magnitude larger than the wavelength of visible light display little wavelength selectivity (unless generated by the light absorptance of specific substances).

The chlorophyll absorption peaks are not particularly apparent in the attenuation spectra even in the phytoplankton-rich waters of Monterey Bay. Theoretical modelling of the optical respone of phytoplankton (Mueller, 1973) indicate that absorption peaks are associated with scattering minima and therefore cancel each other in the attenuation spectra. There is a barely perceptible increase in attenuation at 450 and 650 nm wavelength in the top curve of Fig. 1, but this may be due to diminished scattering in the 0.7° half angle cone of acceptance of the transmissometer. When the transmission is less than 5% forward scattered light may approach the intensity of the transmitted light, thus allowing nonabsorptive bands to transmit relatively more light to the sensor.

Jerlov (1974) shows that the absorption due to yellow matter, a_y, may be calculated by the formula:

$$(C-C_w)_{380} - K(C-C_w)_{655} = a_y$$

where K is determined by the slope of the linear regression of C_{380} and C_{655}. Using this formula and K = 1.4 as determined from our measurements at 400 and 650 nm, we get for the Monterey samples that $a_y = 0$ for the clean water and is negative for more turbid waters. Negative values being unlikely, we must conclude that yellow matter does not play an important role in Monterey Bay. If the major source of yellow mater is continental runoff, then this is a reasonable result as our measurements were taken during a drought and the river mouths were closed due to silt accumulation. Jerlov (1974) computed $a_y = 0.72\ m^{-1}$ in the Baltic where there is abundant

river outflow. This may be an underestimate as our data indicates that K decreases with increasing turbidity and thus constant K cannot be assumed.

Variations with the 30-40% transmission group:

The 30-40% transmission (650 nm) group was chosen because these intermediate values might be found in a wide variety of locations. This group was further subdivided into 6 groups as follows: group 0, sample depth, sd $\geq$ 40 m, water depth, wd > 40 m; group 1, sd < 40 m, wd > 40 m; group 2, sd > 20 m, 20 < wd $\leq$ 40; group 3, sd $\leq$ 20, 20 < wd $\leq$ 40; group 4. Sample closest to bottom, wd $\leq$ 20, group 5, wd $\leq$ 20 except samples nearest bottom. For statistical purposes, this grouping was indicated by 5 variables, at most one of which equalled 1.0, the rest equalled 0.0. A sixth indicator variable was 1.0 for NASA1 stations and 0.0 for NASA2 stations.

A data table containing 61 observations on 13 variables was entered into the Statistical Interactive Programming System (SIPS) as described by Guthrie et al., (1974). These included the five location indicator variables, G_i, the cruise indicator variable, C_r, six particulate beam attenuation values, $C_p(\lambda)$, and the sum of the six attenuation values, C_pT. The six attenuation values were then normalized by dividing by C_pT and standardized by subtracting the mean and dividing by the standard deviation of the normalized attenuation values. Thus, the six resulting attenuation values, C_p', indicate only the spectral shape and each has a mean of 0.0 and a standard deviation of 1.0.

Six new variables are added to the table by multiplying each of the group variables and the cruise variable by C_pT. The new variables we will call CT1 - CT5, CRCT. To demonstrate the use of these new variables lets assume a model of $C_p'(400) = a + bC_pt + cG1 + dCT1$. Now if our sample is not a member of group 1 then $C_p'(400) = a + bC_pT$ since G1 = 0.0 and

$CT1 = G1C_pT = 0$. If our sample is a member of group one then $C_p'(400) = a + bC_pT + cG1 + dCT1$ and since $G1 = 1.0$ that reduces to $a + c + (b + f)\ C_pT$. In other words inclusion of G1 in the model means that the regression equation for C_p vs. C_pT has a different intercept for samples from group 1 than the regression for samples from other groups. Likewise, inclusion of CT1 means that the regression for group 1 has a different slope than the others do.

We would like to know if samples from different cruises and groups have different shaped spectra not related to changes in turbidity. To accomplish this, discriminant analysis (Harris, 1975) is performed. Only 5 of the 6 attenuation values are used since dividing by the sum of the 6 values created a singular matrix (i.e. one column is a linear combination of the other 5 columns). Since were are no longer interested in the change in shape related to turbidity, we first adjust (add to the model, which at this point is just the matrix of means, 0.0) for the sum C_pT of the original six attenuation values. Now the model is $C_p'(\lambda) = K_\lambda t\ A_\lambda C_pT$, where K and A are coefficients which are not given by this method. Instead, we are given the linear combination of the five values ($C_p'(\lambda)$ which is most highly correlated with C_pT. Also given are statistical measures from which one can determine the probability of obtaining a model explaining as much of the variance-covariance as the present one does if the data were a random subset of an infinite set not correlated with C_pT. This probability is found to be much less than 0.01. From the correlations (Table I) of the discriminant function with the six variables $C_p(\lambda)$ we see that as C_pT increases $C_p(450)$ through $C_p(600)$ increases relative to $C_p(400)$ and $C_p(650)$. This is the same sort of variation that we have already observed in Figure 1.

The model is now expanded to include the cruise variable as follows: $C_p'(\lambda) = K(\lambda) + A(\lambda)C_pT + B(\lambda)Cr + D(\lambda)\ CTCr$. Again the coefficients K, A, B and D are not given nor do the K and A necessarily equal K and A for the previous model. The statistics given are now related to the probability of the term $B(\lambda)Cr + D(\lambda)\ CTCr$ removing as much of the variance of $C_p(\lambda)$ as it did if $C_p(\lambda)$ were truly related only (of the present choices) to C_pT. This probability is also less than 0.01. From Table I we see that the

Table I. Discriminant Analysis of $C_p'(\lambda)$ grouped according to cruise, sample depth and water depth; medium turbidity samples

Variables Added	P	Coefficients of discriminant function					Correlation with discriminant function						
		C_p'(400)	450	500	550	600		C_pT	C_p'(400)	450	500	550	600	650
C_pT	<< .01	.125	.221	.138	.147	.201		.708	-.001	.560	.365	.270	.088	-.954
							Cr	CTCr	C_p'(400)	450	500	550	600	650
Cr,CTCr	< .01	.141	-.133	-.083	-.017	.018	-.663	-.660	.614	-.546	-.438	-.168	.013	.340
2nd discriminant function		.212	.191	.096	.151	.228	.168	.183	.315	.475	.156	.220	.067	-.939
							G1	CT1						
G1,CT1	< .07	.073	-.035	.128	.070	.107	.404	.426	-.141	-.538	.696	.262	.410	-.538
G2,CT2 G3,CT3	not significant													
							G4	CT4						
G4,CT4	- .10	.247	.121	.058	.141	.180	.328	.379	.617	.317	.014	.216	-.098	-.8
G5,CT5	not significant													

new discriminant function is negatively correlated with Cr, CTCr and $C_p(450)$ through $C_p(550)$. This means that C_p is relatively higher at the middle wavelengths for NASA1 than for NASA2. This pattern is similar to the correlation pattern for the first model except $C_p(400)$ plays a more important role and $C_p(650)$ plays a less important role than in the first model.

Next the variables associated with the various groups are added sequentially. Only groups 1 and 4 are even marginally significant. Group 1 is the offshore surface waters. From the correlation of the discriminant

function with G1, CT1 and $C_p'(\lambda)$, we see that $C_p'(500)$ is larger relative to $C_p'(400)$, $C_p'(450)$ and $C_p(650)$ for samples from this group than for the others. Group 4 is the inshore bottom samples and these are more spectrally sloped than the samples from the other groups.

From these results we see that ratios of interest for separating groups and cruises are $C_p(450)/C_p(650)$, $C_p(400)/C_p(450)$, $C_p(450)/C_p(500)$, $C_p(400)/C_p(650)$ and $C_p(650)/C_pT$. The primes were dropped from the ratios because the original variables are more understandable and by using ratios the normalization by C_pT is not affected since it cancels out. The normal standardization was used in the discriminant analyses so that each wavelength would be equally weighted in the analysis of variance. This is not a factor in the regression analysis we plan to do.

Multiple regression analysis (Draper and Smith, 1966) is used to find the best (by some criteria) linear models for predicting each of the above ratios from the remaining variables, G1-G5, CR, C_pT, CT1-CT5 and CTCR. The steps taken in each instance are as follows: C_pT is added to the model, if it is significant (F-test) it is kept; the statistical system is asked to add the "best one" of the remaining variables; this is repeated until the variable being added is not significant. At this point all the remaining variables are added. Usually no significant improvement of the model results from this last step and the model used is the one before the addition of the first variable that is not significant. If the additon of all the remaining variables does produce a significant improvement, a table of t-values for each of the coefficients is requested and examined. Those variables judged significant by this t-test then becomes the variables for the model, additions to these are attempted but generally fail the F-test at this point. The results are given in Table II.

As explained before, combining the group coefficients to the constant term and the group-C_pT product coefficients to the coefficient of C_pT, the model can be reduced to the form $y = A + BC_pT$ for each of the groups. The final equations are given on the left side of Table II. On the right side of Table II, the order that the variables are added are given, along with the change in r^2 resulting from the additon of that variable to the model.

TABLE II. Results of multiple regression analysis on chosen spectral attenuation ratios; medium turbidity samples.

$SPM = C_p(450) / C_p(500)$

groups	cruise	regression equation	variable entered	t	p	Δr^2
0,2,3,4,5	1,2	SPM=1.1707				
1	1,2	SPM=1.0886	G1	-3.89	<.001	.204
						.204

$SPE = C_p(400) / C_p(650)$

0,2,3,5	1	SPE=1.2647+.0005 C_pT	C_pT	4.81	<.001	.268
0,2,3,5	2	SPE=.7034+.1326 C_pT	CT4	4.41	<.001	.078
1	1	SPE=1.2647+.0090 C_pT	G4	-4.11	<.001	.145
1	2	SPE=.7034+.1410 C_pT	CTCR	-2.82	< .01	.024
4	1	SPE=-.3575+.3679 C_pT	CR	2.64	<.025	.043
4	2	SPE=-.9188+.4999 C_pT	CT1	1.32	< .20	.014
						.572

$SPME = C_p(450) / C_p(650)$

0,1,2,3,5	1	SPME=1.0748+.0236 C_pT	C_pT	6.09	<.001	.440
0,1,2,3,5	2	SPME=.4977+.1419 C_pT	CT4	2.92	<.005	.041
4	1	SPME=.1929+.2292 C_pT	G4	-2.65	<.025	.056
4	2	SPME=-.3841+.3475 C_pT	CR	3.42	<.005	.034
			CTCR	-3.15	<.005	.065
						.636

$SPSE = C_p(400) / C_p(450)$

groups	cruise	regression equation	variable entered	t	p	Δr^2
0,3,4,5	1	SPSE=1.1805-.0210 C_pT	C_pT	-1.50	<.2	.113
0,3,4,5	2	SPSE=1.2504-.0210 C_pT	CR	-3.92	<.001	.237
1	1	SPSE=1.2045-.0210 C_pT	G2	-1.43	<.2	.040
1	2	SPSE=1.2745-.0210 C_pT	G1	1.38	<.2	.020
2	1	SPSE=1.1419-.0210 C_pT				.410
2	2	SPSE=1.2118-.0210 C_pT				

$SPET = C_p(650) / C_pT$

0,2,3	1	SPET=1.611-.0014 C_pT	C_pT	-6.98	<.001	.454
0,2,3	2	SPET=.2352-.0173 C_pT	CR,CTCR	-4.13	<.001	.087
				4.01	<.001	
1	1	SPET=.1564-.0014 C_pT	CT5	.93	~	.033
1	2	SPET=.2304-.0173 C_pT	G1	-1.79	<.10	.016
4	1	SPET=.2554-.0223 C_pT	CT4	-3.01	<.005	.027
4	2	SPET=.3294-.0382 C_pT	G4	2.87	<.01	.054
5	1	SPET=.1611-.0006 C_pT				.655
5	2	SPET=.2352-.0165 C_pT				

r^2 is the proportion of the variance of the dependent variable about its mean which is predicted by the model. The values given do not necessarily equal the partition of variance in the final model, but do give some idea of the relationship of the models to the unexplained variance. Also given are the t values for each coefficient in the final model and the associated p values. p is the probability of obtaining a coefficient as large as found if the coefficient should really be 0. (Remember our data set should be considered a subset of an infinite data set.)

The first parameter we will study is the ratio $C_p(450)/C_p(500)$. The results of the regression analysis are unique for this ratio as C_pT is not significantly correlated with it. In fact the only significant variable is G1. Thus the t-test reduces to a t-test for the difference of the means (1.1707-1.0886 = .0821) being this large for our sample set if, in fact, offshore surface water does not have a different average $C_p(450)/C_p(500)$ is less than 0.001. Thus, we conclude that the offshore surface water (30-40% transmission at 650 nm) has a lower average ratio of $C_p(450)/C_p(500)$ than water from other locations in Monterey Bay of the same light transmission. Since 450 nm is in the peak of the chlorophyll absorption curve and 500 nm is on the downslope of that same peak, we can guess that perhaps the offshore surface water may have a different combination of phytoplankton pigments than water of equal clarity in other areas. This parameter was also unique in that it didn't seem to vary from the May to the September cruise.

The second ratio under consideration is $C_p(400)/C_p(650)$. The big differences are between cruises and between group 4 and the rest. Substituting an average value of C_pT in the regression equations reveals that

the differences are not so much in the means of the groups but in the slope of the relationship with C_pT. In the first cruise there seems to be little relationship between our ratio and our measure of turbidity C_pT. We only have one sample from cruise 1 group 4, so little can be said about that. However, in cruise 2, in general, and in group 4 (shallow bottom water) especially, there is a relationship between $C_p(400)/C_p(650)$ and C_pT for our medium turbidity group. This parameter being the ratio of the ends of the measured spectra is probably an indication of the overall spectral dependence. If this ratio is more related to total turbidity, C_pT, in one instance than in another, it must mean that the nature of the suspended particulates and dissolved organics is more clearly determined by turbidity in the first case. Cruise NASA2 did not have the complex water structure that NASA1 did. The hydrographic parameters were very uniform down almost as deep as they were measured (90 m) and the frontal structure so obvious during the first cruise was not very apparent. Thus, in this less complicated environment, we may expect more correlation between turbidity and the nature of the suspended particulate matter. Perhaps the importance of group 4 (the shallow bottom samples) is related to the fact that it is the least arbitrarily defined group. While other groups are assigned samples by a discrete boundary in water depth and sample depth, all group 4 samples are within 8 meters of the bottom in shallow water. Not only are the samples in this group less likely to be misassigned but it also has less neighboring groups with which to be mixed. Thus, there is reason to expect that the nature of the particles in this group are also more clearly defined by turbidity.

$C_p(450)/C_p(650)$ behaves very similarly to the parameter just discussed. While this parameter may be more affected by pigmentation the reasoning behind the behavior is identical.

$C_p(400)/C_p(450)$ would be expected to be a pigment effect and similar to $C_p(450)/C_p(500)$. This ratio is just slightly if at all affected by C_pT and consequently is a difference in means rather than slope. However, the significant difference in means is between cruises not groups (if there is a difference between groups it is groups 1 and 2 that are different from each other and the rest, similar to $C_p(450)/C_p(500)$ and contrasted to $C_p(400)/C_p(650)$ and $C_p(450)/C_p(500)$. This behavior is not surprising in itself, but the contrast (cruise vs. group) with $C_p(450)/C_p(500)$ is not readily explainable.

It is not surprising that $C_p(650)/C_pT$ behaves similarly to the other ratios involving $C_p(650)$. It may be surprising that the significance levels for cruise and group 4 are essentially equal to those for the other two parameters. This suggests that 650 nm is important for more than just being the end of the spectrum. Since the parameter is computed by dividing $C_p(650)$ by a sum including itself and spectrally near attenuations, it should be less a measure of spectral dependence than $C_p(400)/C_p(650)$ or $C_p(450)/C_p(650)$. $C_p(650)$ is itself on the edge of a chlorophyll absorption peak and thus perhaps we should not make the difference between overall spectral slope effects and pigment effects as clearcut as was presented in previous paragraphs.

Table II points out in this case that the order of entry into a model is not necessarily the same as the importance in the final model. This is even more apparent when I point out that originally G5 was the first variable added after C_pT but on examining the t-table for the all inclusive model, it was decided to add CR and CTCR first and then repeat the stepwise procedure. This diversion points out that there may be other group effects

not shown in our models that become insignificant when the original sample set is broken up into smaller and smaller groups.

In conclusion, it is found that there are definite differences not related solely to turbidity between samples from different cruises and different locations. The search for the reasons behind these differences will be presented in other sections of this report.

Variation within the 5-20% transmission group

This turbidity group was chosen for its potential for large variability. However, there are fewer samples in this group so the statistical uncertainty is greater. There are no samples from the offshore deep waters on the mid-depth station deep waters and only three samples from the September cruise. The results of the discriminate analysis are given in Table III and the results of the multiple regression analyses is given in Table IV.

Table III. Discriminant analysis of $C_p'(\lambda)$ grouped according to sample depth and water depth; high turbidity samples.

Variables Added	P	Coefficients of discriminant function						Correlation with discriminant function						
		$C_p'(400)$	450	500	550	600		C_pT	$C_p'(400)$	450	500	550	600	650
C_pT	< .025	.404	-.104	-.177	.255	-.128		-.527	.555	.235	-.365	-.090	-.287	-.493
							G3	CT3	$C_p'(400)$	450	500	550	600	650
G3 GT3	> .05	.547	-.201	-.358	.173	.027	-.467	-.519	.706	.313	.000	-.213	-.394	-.618
							G4	CT4						
G4 CT4	> .05	.592	-.077	-.013	.171	.233	.417	.406	.628	.254	-.030	-.113	-.258	-.764
							G5	CT5						
G5 CT5	.05	.452	.023	-.140	-.027	.420	.307	.191	.237	-.066	-.625	.040	.163	-.484

From Table III we see that the most promising parameters to study would be $C_p(400)/C_p(500)$ and $C_p(400)/C_p(650)$. Regression analysis of these parameters produce the results given in Table IV.

Table IV. Regression analysis on chosen spectral attenuation ratios; high turbidity samples.

groups	regression equation	variable entered	t	p	Δr^2
	SPEM = $C_{p(400)}/C_{p(500)}$				
1,5	SPEM = 1.286 - .0146 C_pT	C_pT	-2.33	<.05	.122
3	SPEM = 1.230 - .0146 C_pT	G3	-2.04	.05	.142
4	SPEM = 1.286 - .0101 C_pT	CT4	1.26	<.25	.035
					.299
	SPE = $C_{p(400)}/C_{p(650)}$				
1,3	SPE = 1.282 - .0220 C_pT	C_pT	-2.48	<.025	.077
4	SPE = 1.282 - .0050 C_pT	CT4	3.41	<.005	.194
5	SPE = 1.364 - .0220 C_pT	G5	1.97	<.075	.081
					.352

In contrast with the medium turbidity samples Group 4, the nearshore, near bottom samples have less of a relationship between the spectral parameters and C_pT. This may mean that while the medium turbidity samples from this group had essentially one source, water transported from offshore. High turbidity samples may either originate from the surface layer or resuspended bottom sediments. In this case the variance caused by different sources may mask some of the variance due to changes in turbidity.

Also in contrast with the medium turbidity group in the negative correlation between C_pT and $C_p(400)/C_p(650)$. An explanation is that in the high turbidity region $C_p(400)/C_p(650)$ is decreasing rapidly with increasing turbidity (see Figure 1) while in the medium turbidity range it is almost constant overall (as evidenced by the low slopes for the majority of groups (Table II and the parallelness of the lines in Figure 1b) and has the

contradictory slope for the special case of group 4 and perhaps for the second cruise. In the medium turbidity group 4 may be affected by resuspension of bottom sediment and since the smaller particles are more easily resuspended we might expect $C_p(400)/C_p(650)$ to increase with turbidity because the small particles produce more spectral effect (diameter closer to the wavelength of light). In the high turbidity group we see that group 4 also has a more positive (less negative) slope than the other groups, so that at least, is still consistent with the medium turbidity group.

In conclusion, some variation related to groups and not explainable by total turbidity alone has been found. There is some indication that the slope of the size distribution may play a role. This will be tested in detail in another section. Other auxiallary data will also be examined. It is hoped that the behavior observed in this chapter will be explained when this other data is analyzed.

III. Volume Scattering Functions

The volume scattering functions $B(\theta)$ were measured with a Brice Phoenix Light scattering photometer. The calibration procedures and complete data table for the two Monterey cruises are given by Zaneveld et al (1978). Corrections to the data table are given in an Appendix of this report. The angles, θ, at which $B(\theta)$ was measured are 45, 90 and 135° from the incident beam. The wavelengths, λ, at which measurements were taken are 400, 450, 500 and 550 mm. Thus the scattering of each sample is described by 12 separate parameters.

Variation with turbidity:

The samples were grouped according to the beam transmission of light at 650 nm. wavelength. The variation in angular shape and spectral properties of the volume scattering function between these sample groups are summarized in Table V. $B(45)/B(90)$ for λ=550 nm is relatively constant with just a slight decrease in clear water. $B(45)/B(135)$ for λ=550 nm undergoes a very large change. The high values of $B(45)/B(135)$ in turbid water are consistent with our previous assumption of larger particles since the volume scattering function for large particles is much more peaked in the forward direction than that of smaller particles. The same two parameters computed from tables (Shifrin and Salganik, 1973) are listed in Table VI. Comparison of the two tables shows that the volume scattering function is most similar to the theoretical values for a particle size distribution slope of 4 in turbid water and a slope of 5 in clear water. Perfect comparison is not possible because the tables assume all sizes of particles are spherical, have the same index of refraction and have uniform

index of refraction within the particle. Such is rarely the case but the general size dependency holds true.

Table V: Particle scattering ratios for waters of varying clarity (Bp = B-Bw where Bp is particle scattering and Bw is scattering due to pure water).

	% Tr	$B_p(45)$ m^{-1}	$B_p(45)/B_p(90)$	$B_p(45)/B_p(135)$	$B_p(45)/B_p(45)$	90/90	135/135
λ	650	550	550	550	400/550	400/550	400/550
	5-10	.0384	8.59	12.60	1.21	1.34	1.40
	10-15	.0336	8.39	13.28	1.26	1.24	1.51
	15-25	.0297	8.64	13.46	1.12	1.20	1.52
	25-35	.0216	9.04	11.91	1.14	1.37	1.52
	35-45	.0151	8.79	10.62	1.26	1.51	1.64
	45-55	.0098	8.53	7.94	1.34	1.68	1.76
	>55	.0059	7.88	5.37	1.34	1.80	1.73

Table VI: Theoretical values of scattering ratios for particle size distributions with hyperbolic slope ν and index of refraction m, computed from tables by Shifrin and Salganik (1973).

m	ν	$B_p(45)/B_p(90)$	$B_p(45)/B_p(135)$
1.02	3	20.33	41.20
	4	9.74	14.74
	5	5.32	6.23
1.05	3	10.35	27.78
	4	9.39	15.08
	5	5.40	6.40
1.10	3	3.45	13.74
	4	7.61	14.32
	5	5.43	6.56
1.15	3	10.63	14.53
	4	8.75	13.61
	5	5.50	6.67
1.20	3	12.91	10.65
	4	8.93	11.78
	5	5.51	6.69
1.25	3	13.18	6.83
	4	8.64	9.95
	5	5.47	6.60

The wavelength selectivity for scattering is more pronounced in the clearer waters and for larger angles. For turbid waters, the scattering varies at a rate less than λ^{-1} at 45° about λ^{-1} for 90° and more than λ^{-1} for 135°. In clear water, the scattering varies as λ^{-1} for 45° and varies more than λ^{-1} for 90° and 135°. Again we interpret this to imply that clean water has smaller particles and that the scattering of small particles is more wave length dependent.

Variation within 30-40% Transmission Group:

As in the section II, the 30-40% transmission (650 nm) group was chosen as an intermediate grouping that might include samples from a wide variety of locations. This group was further subdivided into six groups as follows: group 0, sample depth, sd $\geq$ 40 m, water depth, wd > 40 m; group 1, sd < 40, wd > 40; group 2, sd > 20, 20 < wd $\leq$ 40; group 3, sd $\leq$ 20, 20 <wd $\leq$ 40; group 4, sample closest to bottom, wd $\leq$ 20; group 5, samples not closest to bottom, wd $\leq$ 20. For statistical purposes, this grouping was indicated by 5 variables, at most one of which equalled 1.0, the rest equalling 0.0. A sixth indicator variable was 1.0 for NASAI stations and 0.0 for NASA2 stations.

A data table containing 61 observations of 19 variables was entered into the Statistical Interactive Programming System (SIPS) as described by Guthrie et al. (1974). These included the five indicator variables, Gi, the cruise variable, CR, 12 scattering values $B(\theta)\lambda$ (3 angles x 4 wavelengths) and the sum of the 12 scattering values BT. The 12 scattering values were then modified by dividing by their sum and the resulting values were further modified by subtracting the mean of each and dividing by their standard deviations. Thus the 12 new scattering parameters $B'(\theta)\lambda$ indicate only shape and each has a mean of 0.0 and a standard deviation of 1.0.

Six new variables are added to the table by multiplying each of the group variables and the cruise variable by BT. The new variables we will call BT1-BT5, BTCR. As explained in section II, the group indicator variables change the intercept of any model equations, and the product indicator variables change the slope of model equations with respect to BT.

We would like to know if samples from different groups and cruises have different shaped scattering functions (both angularly and spectrally) not related to differences in turbidity. To accomplish this, discriminant analysis (Harris, 1975) is performed. Only 11 of the 12 scattering values can be used since dividing by the sum of the twelve values created a singular matrix (i.e. one column is a linear combination of the other 11 columns). Since we are no longer interested in the change in shape related to turbidity, we first adjust (add to the model, which at this point is just the matrix of means, 0.) for the sum of the original (unnormalized) 12 scattering values, B_t. Now the model is $B'(\theta)_\lambda = K(\theta)_\lambda + A(\theta)_\lambda$ BT, where K and A are coefficients which are not given by this method. Instead we are given the linear combination (discriminant function) of the 11 values $B'(\theta)_\lambda$ which is most highly correlated with BT. Also given are statistical measures from which one can determine the probability of obtaining a model explaining as much of the variance as this one if the data were a random subset of an infinite set not correlated with Bt. This probability is found to be much less than 0.01.

The model is now expanded to include the cruise variables as follows: $B'(\theta)_\lambda = K(\theta)_\lambda + A(\theta)_\lambda$ BT + $C(\theta)_\lambda$ CR + $D(\theta)_\lambda$ BTCR. Again the coefficients K, A, C, and D are not given. The statistics given are now related to the probability of the terms $C(\theta)_\lambda$ CR and $D(\theta)_\lambda$ BTCR removing as much of the variance of $B(\theta)_\lambda$ as they did if $B(\theta)_\lambda$ were truely only related to Bt. This probability

is found to be slightly less than 0.01. The method provides two orthogonal linear combinations of $B(\theta)_\lambda$, the first of which maximizes the correlation with CR and BTCR and the other removing the maximum portion of the remaining variance.

Similarly the variables associated with the various groups are added sequentially. Table VII gives the statistical test values, the coefficients of the discrimenant functions and the correlation coefficients of the discriminant functions with the values $B'(\theta)_\lambda$.

Table VII: Multivariate analysis of variance of $B'(\theta)_\lambda$ adjusted for Bt and grouped according to cruise, sample depth and water depth; medium turbidity samples.

Variables added:

BT $\lambda = 3.10$ $F = 10.71$ with 11 and 38 d.f.

$p << .01$

Discriminant Function

	coefficients				correlation with BT -.72		
λ/θ	45	90	135	λ/θ	45	90	135
400	-.148	-.084	.101	400	-.13	.60	.91
450	-.217	-.024	-.109	450	-.38	.26	.90
500	-.169	-.108	.046	500	-.67	-.26	.87
550	-.218	-.085		550	-.57	.30	.77

CR, BTCR $\lambda = 2.43$ $\theta = .708$

$s = 2$ $m = 4$ $m = 18$ $p < .01$

First Discriminant Function

	coefficients				correlations		
					CR -.67	BTCR -.63	
λ/θ	45	90	135	λ/θ	45	90	135
400	.035	.018	.182	400	-.04	.67	.90
450	-.008	.012	-.034	450	-.24	.32	.89
500	-.046	-.087	.061	500	-.78	-.35	.78
550	-.043	.049		550	-.63	.38	.72

Second Discriminant Function

	coefficients				correlations		
					CR .33	BTCR .32	
λ/θ	45	90	135	λ/θ	45	90	135
400	-.152	.058	-.032	400	-.55	.47	.14
450	-.052	-.067	-.149	450	-.11	.23	.15
500	-.067	-.062	-.046	500	-.03	.62	.18
550	-.180	.061		550	-.21	.58	.23

G1, Be 1
G2, Bt 2 - not significant

G3 $\lambda = .609$ $F = 2.10$ with 11 and 38 d.f. $p = .05$

Discriminant Function

	coefficients				correlations		
					G3 -.40		
λ/θ	45	90	135	λ/θ	45	90	135
400	.230	.073	.078	400	.39	-.49	-.40
450	.240	.034	.109	450	.45	-.47	-.53
500	.138	.072	.122	500	.28	-.06	-.42
550	.318	-.060		550	.36	-.85	-.76

G4, Bt 4
G5, Bt 5 - not significant

The interpretation of the coefficients and correlations is not straight forward. In general, though, the discriminant function for BT contrasts 45° against the other two angles and there is some indication of a contrast between 400 nm and the rest of the wavelengths except at 135°. Since BT is negatively correlated with the discriminant function, this indicates that more turbid waters have steeper sloped scattering functions in the forward direction and lower ratios of scattering at 400 nm vs longer wavelengths. This is consistent with the results at the beginning of this section (Table V) for all the scattering samples versus transmission groups.

By examining the contrasts between the correlation coefficients of the discriminant functions for differing wavelength and angle, five parameters characterizing important changes in spectral and angular shape have been chosen. These are: SP4=B(45)400/B(45)500 , SP9=B(90)400/B(90)500, SP13=B(135)400/B(135)550 , SH9=B(45)550/B(90)550 and SH13=B(45)500/B(135)500. Multiple Regression Analysis (Draper and Smith, 1966) will be used to investigate the relationship of these parameters with group and cruise variables. Multiple regression analysis finds the best (by some criteria) linear models for predicting each of the five variables SP4-SH13 from the remaining variables G1-G5, BT, CR, BTCR, BT1-BT5. The steps taken in each instance are as follows: BT is added to the model, if it is significant it is kept; the system is asked to add the "best one" of the remaining variables; this is repeated until the variable being added is not significant. At this point all the remaining variables are added. Usually, no significant improvement of the model results from this last step and the model used is that before the addition of the first variable that is not significant. But if the addition of all the remaining variables does produce a significant improvement, a table of t-values for each of the coefficients is

requested and examined. Those variables judged significantly by this t-test then become the variables included in the model. Additions to these are attempted but generally fail to be significant (F-test). The results are given in Table VIII. The explanation of the items in Table VIII are equivalent to those given for Table II in Section II.

Table VIII: Regression Analysis of chosen scattering ratios as a function of the summation of the scattering values for samples grouped according to sample depth and water depth; medium turbidity samples.

groups	cruise	regression	variable added	t	p	Δr^2
		SP4 = B(45)400/B(45)500				
0,1,2,3	1	SP4=1.025+ .461 BT	BT	-2.88	< . 01	.077
0,1,2,3	2	SP4=1.332-1.664 BT	CR	-4.51	< .001	.234
4	1	SP4=1.025- .016 BT	G5	3.16	< .005	.106
4	2	SP4=1.332-2.141 BT	BTCR	3.13	< .005	.077
5	1	SP4=1.121+ .461 BT	BT4	-1.54	< . 20	.021
5	2	SP4=1.428-1.664 BT				.515
		SP9 = B(90)400/B(90)500				
0,1,3,5	1	SP9=1.223+ .450 BT	BT	-4.87	< .001	.148
0,1,3,5	2	SP9=2.320-8.617 BT	CR	-5.16	< .001	.141
2	1	SP9=1.057+ .450 BT	BTCR	4.34	< .001	.177
2	2	SP9=2.155-8.617 BT	G2	-1.73	< . 10	.025
4	1	SP9=1.089+ .450 BT	G4	-1.34	< . 20	.016
4	2	SP9=2.187-8.617 BT				.507
		SP13 = B(135)400/B(135)550				
0	1,2	SP13=1.930+9.734 BT	BT	2.86	< . 01	.048
1	1,2	SP13=1.930- .823 BT	BT1	-3.38	< .005	.006
2	1,2	SP13=1.930-3.549 BT	BT2	-3.00	< .005	.015
3	1,2	SP13= .805+9.734 BT	BT5	-2.99	< .005	.025
4	1,2	SP13=1.930-2.567 BT	BT4	-2.95	< .005	.052
5	1,2	SP13=1.930-2.338 BT	G3	-2.87	< . 01	.113
						.259
		SH9 = B(45)550/B(90)550				
0,2,3	1	SH9=9.266- 4.941 BT	BT	5.20	< .001	.060
0,2,3	2	SH9=1.127+64.14 BT	G4,BT4	3.17 -1.68	< .005 < . 10	.016
1	1	SH9=12.44-22.57 BT	BT1	-1.71	< . 10	.026
1	2	SH9=4.297+46.51 BT	CR	6.58	< .001	.042
4	1	SH9=13.89-26.94 BT	BTCR	-6.03	< .001	.239
4	2	SH9=5.750+42.14 BT	G5	3.59	< .001	.049
5	1	SH9=15.86-55.04 BT	BT5	-2.96	< .005	.036
5	2	SH9=7.793+14.04 BT	G1	2.75	< . 01	.069
						.537
		SH13 = B(45)500/B135)500				
0,3,4,5	1	SH13=8.654+22.48 BT	BT	5.51	< .001	.400
0,3,4,5	2	SH13=1.437+72.53 BT	CR	4.68	< .001	.066
1	1	SH13=9.673+22.48 BT	BTCR	-3.60	< .001	.087
1	2	SH13=2.456+72.53 BT	G1	2.15	< . 05	.048
2	1	SH13=8.654+ 7.639 BT	BT2	-1.30	< . 20	.012
2	2	SH13=1.437+62.70 BT				.613

The unexplained variance is large (39-74% of the original variance). It would not be so large if we hadn't limited our samples to a small range of turbidity, effectively decreasing our signal to noise ratio. Nor is this surprising to those of us familiar with the instrument and its operation, there are many sources of experimental error. Of course, some of the remaining variance could be due to differences in optical properties between samples in the same group due to factors we haven't considered yet and factors we have not even measured.

The relationship between turbidity and the spectral and angular shape of the scattering function is much stronger during NASA2 than during NASA1. In addition NASA1 displays increasing spectral dependence and lesser sloped forward scattering with increasing turbidity in contrast to both NASA2 and the total data set (not restricted by transmission limit), which show decreasing, spectral dependence and steeper sloped forward scattering with increasing turbidity. During NASA1 samples with transmission values in this group (30-40%) were characteristic of transition zones between the clear waters and the surface productive waters while waters of the same clarity were representative of the entire mixed layer for NASA2. Thus, while the more turbid water within the 30-40% Transmission range has slightly higher average particle size, during NASA1 there may also be a large decrease in index of refraction resulting in optically smaller particles. This would also explain why samples from group 4, the shallow near bottom samples, display practically no relationship to BT for NASA1 but a very strong negative relationship during NASA2. The high index particles from the bottom could cancel the effects of the low index phytoplankton for NASA1 and overwhelm the phytoplankton for NASA2. Group 5, the shallow water samples display higher average spectral ratios and forward scattering ratios. This could be due to a higher inorganic

component attributed to its proximity to the bottom and the shore or it could denote a different assemblage of phytoplankton species than water farther offshore. The possibility of this and the other relationships being explained by particle size distributions and pigments will be examined in a later section.

Variation within 5-20% transmission group:

This turbidity group was chosen for its potential for large variability. However, there are fewer samples in this group so the statistical uncertainty is greater, there are no samples from the offshore deep waters or the mid-depth station deep waters, and only three samples from the September cruise. The results of the discriminate analysis are given in Table IX and the results of the multiple regression analysis is given in Table X.

TABLE IX: Discriminant analysis of $B'(\theta)_\lambda$ adjusted for Bt and grouped according to sample depth and water depth; high turbidity samples.

Two largest characteristic roots: λ = 1.188, .643
Associated test statistics $\theta = \frac{\lambda}{1+\lambda}$ = .543, .391 s=3 m=$3^1/_2$ n=12
resulting p for first root p < .10

First discriminant function

coefficients of $B'(\theta)_\lambda$				correlation of discriminant function with $B'(\theta)_\lambda$			
λ/θ	45	90	135	λ/θ	45	90	135
400	-.406	-.215	.011	400	.12	.09	-.43
450	-.465	-.094	-.312	450	-.11	.22	-.42
500	-.548	-.046	-.177	500	-.26	.49	-.29
550	-.255	.154		550	.44	.78	-.16

Second discriminant function

	coefficients				correlations		
λ/θ	45	90	135	λ/θ	45	90	135
400	.026	.017	-.135	400	.21	.31	.15
450	-.250	.005	-.374	450	-.20	-.20	-.11
500	.038	-.118	.374	500	-.12	-.06	.30
550	-.156	-.001		550	.12	.19	.00

TABLE X: Results of Multiple Regression Analysis on chosen spectral and angular shape factors; high turbidity samples.

Groups represented	Final regression equation	Predicted value	Variable entered	t	p	Δr^2
		$SP4 = B(45)_{400}/B(45)_{500}$				
1,4,5	SP4=1.098	1.098	----	----	----	----
3	SP4= .880+2.844 BT	1.164	BT3, G3	2.34,-1.65	<.05,.15	.096,.096
						.165
		$SP9 = B(90)_{400}/B(90)_{500}$				
1,3,4	SP9=1.337-1.467 BT	1.191	BT	-1.940	<.06	.045
5	SP9=1.337- .202 BT	1.317	BTS	2.002	<.06	.103
		$SP13 = B(135)_{400}/B(135)_{500}$				
1	SP13=1.466	1.466	----	----	----	----
3	SP13=1.466-2.612 BT	1.205	BT3	-3.644	.001	.161
5	SP13=1.283	1.283	G5	-2.265	<.05	.061
4	SP13=1.263	1.263	G4	-1.860	<.10	.076
						.298
		$SH9 = B(45)_{400}/B(90)_{400}$				
1,3,4,5	SH9=7.454	7.454	----	----	----	----
		$SH13 = B(45)_{400}/B(135)_{400}$				
1,4,5	SH13=6.944+23.42 BT	9.286	BT	3.080	<.10	.251
3	SH13=6.944+34.25 BT	10.37	BT3	1.620	<.15	.055
						.306

Common to both turbidity groups is the importance of the 135° scattering measurements. This is not surprising, in that the shape of backscattering curves varies more with the size and index (Morel, 1973) and with the shape (Gibbs, 1978) than the forward scattering does. It is also consistent with our own observations that there is more spectral dependence at 135° than 45°. The actual factors producing the difference between the scattering functions for different sample location groups can only be guessed at this point.

IV. PARTICLE SIZE DISTRIBUTIONS AND PIGMENT PARAMETERS

In previous sections it has been shown that the spectral shape of attenuation and scattering is statistically different in waters of the same clarity but different location and different season. In this section we will test the hypothesis that these differences between location groups and between cruises can be explained by differences in particle size distributions.

Six new parameters, P_i', will be introduced to our multivariate model. $P_i' = P_i/(\sigma_i \Sigma(P_i/\sigma_1))$ where P_1 is the number of particles per milliliter with spherical equivalent diameters between roughly 2.5 and 4.0 and P_2 through P_6 cover respectively diameters from 4.0-6.2, 6.2-10, 10-16, 16-25 and 25-40 μm. σ_i is the standard deviations of P_i about its mean.

The results of the multivariate analyses of variance are given in Table XI. In contrast to our expectations, the cruise and group effects are just

TABLE XI: Multivariate analysis of variance of Cp'(λ) grouped according to cruise, sample depth and water depth, and as a function of particle size distribution, medium turbidity samples.

Variables Added	P	Coefficients of Discriminant Function					Correlation with Discriminant Function						
		Cp'(400)	450	500	550	600	CpT	Cp'400	450	500	550	600	650
CpT	<<.01	.169	.256	.149	.169	.235	.72	.10	.58	.32	.24	.05	-.96
P_1'-P_5'	<.01	.310	.088	-.038	.049	.143		.88	.30	-.33	-.18	-.25	-.34
								P_i	2	3	4	5	6
								.36	.27	-.38	-.36	-.34	-.09
		.006	.220	.098	.054	.049		-.02	.87	.34	.05	-.26	-.68
								P_i	2	3	4	5	6
								.34	.52	-.18	-.54	-.27	-.36
CR,CRCT	<.01	.320	.081	-.022	.047	.147		.90	.27	-.27	-.20	-.24	-.36
								CR	-.33	CRCT		-.33	
		.114	.229	.151	.176	.230		-.12	.46	.36	.35	.19	-.94
								CR	.42	CRCT		.43	
G1, CT1 G2, CT2 G3, CT3	----	Not Significant											
G4, CT4	<.05	.342	.122	.026	.113	.193		.82	.31	-.14	-.02	-.21	-.59
								G4	.35	CT4		.40	
G5, CT5	----	Not Significant											

as important after adjusting the model for the particle size distribution shapes as they were in section II where the particle effect was not included. The particle size distribution shape is also important. Thus differences in spectral shape of the particulate attenuation spectra between groups is not totally explained by differences in the particle size distribution. On the contrary, after adjusting for the particle effect, the inshore near-bottom samples are, if anything, more statistically different from the rest.

Contrasting correlations in Table XI suggests two new spectral parameters to study Cp(400)/Cp(500) and Cp(400)/(Cp(500) + Cp(650)) and two particle parameters PES=P1/(P3+P5) and PMM=P2/P4. Continuing the same sequence as in section II, the previously studied spectral parameters plus the two new ones will be subjected to regression analysis including particle size distribution parameters in addition to the group and cruise parameters used previously. The results of this analysis are compared with the results from section II in Table XII.

Group 4 has decreased in importance somewhat but Group 1 is more strongly related to the particulate attenuation spectral shape adjusted for particle size distributions shape than it was to the attenuation not adjusted for particles. The coefficients pertaining to CpT and cruise have also become more significant and the particle size distribution parameters are very important also, especially P2'. The percent of total variance removed, r^2, has also increased significantly (from 40-65% to about 75% in the case of SPE, SPME and SPSE). Thus instead of finding that the relationships in Section II are caused by differences in the particle size distributions, we find that the

TABLE XII: Comparison of regression analyses on particulate attenuation spectral parameters with and without particle size distribution shape parameters.

WITHOUT				WITH			
Variable entered	t	p	r^2	Variable entered	t	p	r^2
SPM = Cp(450)/Cp(500)							
G1	-3.89	<.001	.204	G1	-3.76	<.001	
				PES	1.49	<.2	
				CR	-2.22	<.05	
				P2'	2.27	<.05	
				PMM	-1.44	<.2	.329
SPE = Cp(400)/Cp(650)							
CpT	4.81	<.001		CpT	5.05	<.001	
CT4	4.41	<.001		CT4	3.24	<.005	
G4	-4.11	<.001		G4	-3.22	<.005	
CTCR	-2.82	<.01		P2'	5.00	<.001	
CR	-2.64	<.025		CTCR	-4.24	<.001	
CT1	1.32	<.20	.572	CR	3.43	<.005	
				G1	1.78	<.10	
				P1'	3.59	<.001	
				P5'	3.42	<.005	
				PMM	-2.40	<.025	
				CT1	-1.43	<.20	.746
SPME = Cp(450)/Cp(650)							
CpT	6.09	<.001		CpT	7.19	<.001	
CT4	2.92	.005		P2'	4.49	<.001	
G4	-2.65	<.025		CT4	2.43	<.025	
CR	3.42	<.005		G4	-2.33	<.025	
CTCR	-3.15	<.005	.636	P5'	2.97	<.005	
				P1'	2.98	<.005	
				P4'	2.85	<.01	
				CTCR	-4.08	<.001	
				CR	3.90	<.001	.751
SPSE = Cp(400)/Cp(450)							
CpT	-1.50	<.20		CpT	5.05	<.001	
CR	-3.92	<.001		CT4	3.24	<.005	
G2	-1.43	<.20		G4	-3.22	<.005	
G1	1.38	<.20	.410	CTCR	-4.24	<.001	
				P2'	5.00	<.001	
				CR	3.43	<.005	
				G1	1.78	<.10	
				P5'	3.42	<.005	
				P1'	3.59	<.001	
				PMM	-2.40	<.025	
				CT1	-1.43	<.20	.746

TABLE XII (con't)

SPET = Cp(650)/CpT

Without				With			
Variable entered	t	p	r^2	Variable entered	t	p	r^2
CpT	-6.98	.001		CpT	-7.63	.001	
	-4.13	.001			-4.61	.001	
CR, CTCR	4.01	.001		CR, CTCR	4.88	.001	
CT5	.93	----		P2	-3.74	.001	
G1	-1.79	.10		PMM	2.83	.01	
CT4	-3.01	.005		G1	-2.22	.05	
G4	2.87	.01	.655	CT1	1.82	.10	
				P1	-2.01	.05	
				P5	-1.85	.10	.689

SPEM = Cp(400)/Cp(500)

CpT	-2.09	.05	
CR	-6.21	.001	
PES	4.11	.001	
P2	3.76	.001	
P6	2.83	.01	
G1	-2.43	.025	.581

SPES = Cp(400)/(Cp(500) + Cp(650))

CpT	-4.22	.001	
P2	6.46	.001	
CTCR	-2.56	.025	
P1	5.90	.001	
P5	2.56	.025	
PMM	-3.51	.001	
P6	2.57	.025	
G2	-1.73	.025	
CR	1.34	.20	.686

effect of the particle size distributions has been partly obscuring other effects (nature of particles, dissolved substances) related to group and cruise. The high significance of P2' and positive t value (thus positive coefficient) indicates that the small particles do tend to increase the spectral effect although P5' is also positive (to a lesser degree) indicating perhaps some special species that is strongly absorbant in the short wavelength region.

The two new parameters SPEM = Cp(400)/Cp(500) and SPES = Cp(400/(Cp(500) + Cp(650)) are influenced to only a very small amount by groups. This indicates that some parameters are less sensitive to effects other

than particle size distribution and thus might be good predictors of particle size distributions. Conversely, SPM = Cp(450)/Cp(500) is only weakly related to Gl, the offshore surface water.

Introducing our six new parameters Pi' into the multivariate analysis of variance for scattering produces the results given in Table XIII.

TABLE XIII. Multivariate analysis of B'(θ)λ adjusted for BT and particle size distribution shape and grouped according to cruise, sample depth and water depth, medium turbidity samples.

Variable Added BT F=11.31 t <<.01

Discriminant function

	coefficients				correlations		
λ \ θ	45	90	135	λ/θ	45	90	135
400	.169	-.103	.106	400	-.05	.59	.89
450	-.285	-.040	-.152	450	-.43	.23	.89
500	-.205	-.113	.037	500	-.62	-.23	.88
550	-.293	-.110		550	-.60	.28	.76

P1'-P5' S=5 m=2.5 n=15.5

p<.05

First Discriminant Function

	coefficients				correlations					
					P1'	P2'	P3'	P4'	P5'	P6'
					-.13	-.19	.05	.35	.01	.13
λ \ θ	45	90	135	λ/θ	45	90	135			
400	.039	.035	.229	400	-.08	.68	.89			
450	-.005	.037	-.047	450	-.33	.34	.88			
500	.032	-.118	.107	500	-.72	-.33	.81			
550	-.015	.082		550	-.62	.42	.74			

TABLE XIII. (con't)

Second Discriminant Function

	coefficients			correlations			
				P1'	P2'	P3'	P4'	P5'	P6'
				.45	.03	-.13	-.28	-.26	-.09
λ \ θ	45	90	135	λ/θ	45	90	135		
400	.214	.070	.182	400	-.52	-.10	-.09		
450	.458	.104	.174	450	.46	.10	-.11		
500	.255	.070	.144	500	-.30	.02	-.23		
550	.463	.278		550	.33	.37	-.13		

CR, BTCR S=2 m=4 n=15.5 p<.01

First Discriminant Function

	coefficients			correlations			
				CR .64	BtCR .60		
λ \ θ	45	90	135	λ/θ	45	90	135
400	-.015	-.010	-.194	400	.03	-.67	-.90
450	.036	.017	.077	450	.28	-.28	-.89
500	.084	.072	-.053	500	.78	.26	-.82
550	.100	-.062		550	.65	-.43	-.74

Second discriminant function

	coefficients			correlations			
				CR .37	BTCR .43		
λ \ θ	45	90	135	λ/θ	45	90	135
400	.152	.214	.052	400	-.62	.31	-.06
450	.373	.089	.208	450	.18	.31	-.01
500	.345	.064	.090	500	0	.32	-.19
550	.336	.273		550	.03	.53	-.05

G1, Bt1
G2, Bt2 -- not significant G3 F=2.07 with 11 and 33 d.g. freedom
P= .05

Discriminant function

	coefficients				correlation G3 .35		
θ	45	90	135	λ/θ	45	90	135
λ							
400	-.157	-.041	-.048	400	-.36	.49	.49
450	-.135	-.038	-.023	450	-.41	.43	.62
500	-.274	-.091	-.042	500	-.36	-.04	.53
550	-.205	.128		550	-.44	.84	.80

G4 BT4
G5 BT5 -- not significant

Study of the correlation tables suggest these parameters $B(45)_{400}/B(45)_{500}$, $B(90)_{400}/B(90)_{500}$, $B(45)_{500}/B(135)_{500}$, $B(45)_{550}/B(90)_{550}$ and $B(135)_{400}/B(135)_{550}$. These particle ratios are suggested by the tables P_2/P_4 and $P_1/(P_4+P_5)$. While the particle parameters were significant at the .05 level, the significance of cruise and group 3 were not changed from the model without the particle parameters (section III). In fact the F value for group 3 was almost exactly the .05 critical level for both models. Bt3 is not used because it is .99 correlated with G3 and creates a nonsingular matrix of both are included.

From the comparison of the Regression Analysis (Table XIV) with and without the particle size distribution shape parameters, it is evident that the size distributions add nothing to the spectral shape of the scattering functions, little to the backward scattering and just moderately to B(45)/B(90). This leads to two hypotheses, either the size distributions contribute little to the spectral shape of the scattering, or what they contribute is explained equally well by the other parameters. These hypotheses were further tested on SP4 by replacing various independent parameters in the final model with the particle size parameters. Replacing the group parameters G5 and BT4 with he particle parameters only reduced the total percent of variance explained from 51.8% to 49%. Replacing the cruise parameters CR and BTCR instead

reduced the variance removed from 51.8% to 47.6%. Finally replacing parameters pertaining to the summation of the scattering values BT, BT4, BTCR raised the percent of variance explained from 51.8% to 52.3%. However, using only the particle variables removed only 20.6% of the total variance of SP4. Thus, we conclude that the particle size distribution shape parameters explain the same variance as BT and related terms (BTCR, BT4) or having already adjusted for BT can explain some of the variance due to differences between cruises and groups.

TABLE XIV; Comparison of Regression Analysis of the volume scattering function $B(\theta)_\lambda$ with and without the particle size distribtution parameters P_i', medium turbidity samples.

			$SP4 = B(45)_{400}/B(45)_{500}$				
Variable entered	t	p	r^2	Variable entered	t	p	r^2
BT	-2.88	<.01		BT	-2.86	<.01	
CR	-4.51	<.001		CR	-4.50	<.001	
G5	3.16	<.005		G5	3.16	<.005	
BTCR	3.13	<.005		BTCR	3.12	<.005	
BT4	-1.54	<.20	.515	BT4	-1.51	<.20	.518
			$SP9 = B(90)_{400}/B(90)_{500}$				
BT	-4.87	<.001		BT	-4.86	<.001	
CR	-5.16	<.001		CR	-5.15	<.001	
BTCR	4.34	<.001		BTCR	4.34	<.001	
G2	-1.73	<.10		G2	-1.37	<.20	
G4	-1.34	<.20	.507	G4	-1.33	<.20	.492
			$SP13 = B(135)_{400}/B(135)_{550}$				
BT	2.86	<.01		BT	2.81	<.01	
BT1	-3.38	<.005		BT1	-3.36	<.005	
BT2	-3.00	<.005		BT4	-2.94	<.005	
BT5	-2.99	<.005		BT5	-2.98	<.005	
BT4	-2.95	<.005		BT2	-2.91	<.01	
G3	-2.87	<.01	.259	G3	-2.86	<.01	.261

TABLE XIV. (con't)

SH9 = $B(45)_{550}/B(90)_{550}$

Variable entered	t	p	r^2	Variable entered	t	p	r^2
BT	5.20	<.001		BT	5.87	<.01	
G4,BT4	3.17,-1.68	<.005		P5'	3.19	<.005	
		<.10					
BT1	-1.71	<.10		CR,BTCR	6.39,-6.13	<.001	
CR	6.58	<.001		P6'	-2.47	<.025	
BTCR	-6.03	<.001		G3	-2.57	<.025	
G5	3.59	<.001		G2	-2.60	<.025	
BT5	2.96	<.005		BT3	2.20	<.05	
G1	2.75	<.01	.537	G4	2.59	<.025	
				G5,BT5	2.59,-2.56	<.025	.620

SH13 = $B(45)_{500}/B(135)_{500}$

BT	5.51	<.001		BT	4.72	<.001	
CR	4.68	<.001		CR	4.08	<.001	
BTCR	-3.60	<.001		BTCR	-2.63	<.025	
G1	2.15	<.05		P2'	-1.87	<.10	
BT2	-1.30	.20	.613	BT1	2.17	<.05	.637

The parameter SH9 shows a moderate increase in the amount of total variance removed upon addition of the particle parameters P5', P6' (Table). Also shown is a shift from groups 1, 4, and 5 to groups 2, 3, 4, 5. Replacing the parameters G2, G3, BT3, with the parameters G1, BT1 and BT4 reduces r^2 from .620 to .616 which is not at all significant. Replacing BT, BTCR, BT1, BT4 BT5 with the rest of the particle parameters reduces r^2 from .616 to .289, and replacing G1, BT1, G4, BT4, G5, BT5 with the particle parameters reduces r^2 from .616 to .384. Thus it is seen that for the angular shape of the scattering functions the particle size distribtution explains variance in addition to that explained by BT, cruise and groups but explains little of the variance due to BT, cruise and groups.

In summary, the shape of the particle size distribution explains much addition variance of the spectral shape of the attenuation curve, a little addition variance of the angular shape of the scattering function and very little additional variance for the spectral shape of the scattering function.

On the other hand, groups and cruise always explains variance in addition to what is explained by the particle information while BT explains little of the variance in the spectral shape of scattering beyond what is explained by particles group and cruise.

Attenuation, spectral scattering shape and angular scattering shape are all affected by not only the size of the particles but also their nature. However, angular scattering shape (especially at 135°) is highly affected by the shape of the particle (Gibbs, 1978) while attenuation may be strongly affected by differences in pigmentation and dissolved substances. Spectral shape of scattering may be less affected by particle shape and pigmentation and not at all by dissolved substances. This may explain why the particle size distribution information is more in common with the turbidity group and cruise information for the spectral shape scattering parameters than it is with the same information for the angular shape scattering parameters and the spectral shape attenuation parameters.

Biological Parameters:

Also measured during these cruises were chlorophyll a, phaeophytin, and particulate carbon and nitrogen. They are entered into the regressions in the following forms: ORG = CHL + PHE, PCO = ORG/VOL, PCU = PHE/ORG, CN = C/N where CHL is chlorophyll a concentration, PHE is phaeophytin concentration, VOL is total particulate volume as determined by the electronic particle sizer and C and N are particulate carbon and nitrogen concentrations, respectively. The parameter CN was soon discarded because of a large amount of missing data points and a poor correlation with other parameters apparently due to large experimental errors. Also included

in the possible regression parameters are the suspended particulate volume concentrations (VOL), the slopes (SLP) of the particulate size distributions and the particle concentrations in the size classes P0-P6.

The first parameter to be examined is SPM = $C_p(450)/C_p(500)$. Values of SPM greater than 1.5 were discarded because they were due to spectral uncertainty of Cw and of the calibration for samples from the very clear water. Because most parameters are highly correlated with VOL, the interpretation of a model including VOL would be ambiguous. Table XV gives the correlation coefficients between various parameters pertinent to the understanding of the behavior of the regression sequence about to be described.

VOL would be added first in the standard STEPWISE (Guthrie et al., 1974) routine, but as stated above, this is ambiguous. Optical parameters are usually predicted theoretically by the slope of the size distribution and by the relative index of refraction of the particles (Shiffin and Salganik, 1973). Therefore, SLP is added first and since there is a high correlation between SLP and VOL, VOL now is significant in explaining

TABLE XV

CORRELATION COEFFICIENTS (X100) BETWEEN PARAMETERS PERTINENT TO THE PREDICTION OF SPM = $C_p(450)/C_p(500)$ for NASA1

SPM	X						
SLP	56	X					
PCO	20	4	X				
P2	-12	38	-19	X			
ORG	-36	-51	45	-14	X		
PCU	- 8	-11	35	- 4	28	X	
P5	-59	-79	- 9	-13	63	20	X
VOL	-61	-67	-14	18	64	16	94
	SPM	SLP	PCO	P2	ORG	PCU	P5

residual variance only at the 10% probability level. The additional parameters that are significant at the 5% level, at least in combination, are P2, ORG, and PCO. A model including these three parameters plus SLP is arrived at using both forward (after SLP is added) and backward stepping in the regression routine. Of these we would expect PCO to be most indicative of index of refraction, P2 might indicate a particular species or general type of suspended particle, and ORG would indicate the overall level of biological activity. To examine the relationships between these parameters, they have been added in the above order and the changes in the t-values of their coefficients are examined in Table XVI.

TABLE XVI

T-VALUES FOR THE REGRESSION EQUATIONS
PREDICTING SPM = $C_p(450)/C_p(500)$ for NASA1

	t-values				r^2
VARIABLE	SLP	PCO	P2	ORG	
	7.79				.318
	7.84	2.52			.350
	9.79	1.54	-4.96		.455
	6.33	2.71	-4.33	-2.48	.480

Adding PCO does not affect the t-value for SLP significantly, leading to the conclusion that they are relatively independent effects as verified by their low correlation in Table XV. Adding P2, however, increases the importance of SLP and decreases the importance of PCO. The correlation between SLP and P2 is only 0.38 while the correlation between SLP and P5 is -0.79. Thus SLP generally indicates a change in the number of large particles while the small particles display much smaller changes. Table XVI indicates that if the increase in SLP for a particular sample is due

to an increase in small particles especially those of the size of P2 rather than the more common decrease in the number of large particles than the ratio SPM = $C_p(450)/C_p(500)$ does not increase as much as if the large particles had changed. Furthermore, as the large particles are positively correlated with ORG and the small particles have a slightly negative correlation with ORG, SLP and P2, being almost directly related to both P5 and VOL, explain some of the variance originally accounted for by PCO = ORG/VOL. This is further verified by the fact that adding ORG to the model reduces the importance of SLP and P2 and increases the importance of PCO. However, all four are still significant at the 5% level which may mean each contains some independent information or perhaps implies an averaging process that eliminates some experimental error thus allowing four parameters to do a better job of describing two processes than two parameters alone could do. The r^2 column of Table XVI shows that four parameters remove 13% more of the variance than two parameters do. Not shown is the SLP, P2 combination which removes 44.5% of the variance. Thus, the averaging concept is very plausible in that it would only remove an additional 3 1/2% of the variance.

SPE ($C_p(400)/C_p(650)$) behaves much the same as SPM except that SLP is much more important, explaining 53% of the variance while three additional parameters only remove an additional 8%. Also P3 is chosen instead of P2, but is not quite significant at the 5% level. Furthermore, PCO is not significant in itself but only in combination with ORG. Total suspended volume is also more important as it is still preferred after SLP is added, but is not included in the model arrived at by backstepping. The additional importance attached to volume may explain why PCO is not significant in itself but is in combination with ORG as PCO = ORG/VOL.

SPME ($C_p(450)/C_p(650)$) behaves differently in that ORG does not enter into the final regression. SLP removes 37% of the variance and PCO and P5 together remove an additional 5% of the variance. As in the previous two parameters adding PCO does not reduce the t-value for the coefficient of SLP. Thus, there appears to be two independent effects, the size distribution and something related to PCO, $(\frac{CHL + PHE}{VOL})$. The size distribution appears to be the dominant factor although another possibility is that PCO is only a mediocre indicator of the other factor which may be the index of refraction distribution (index of refraction includes absorption spectra).

One parameter that is an exception is SPSE ($C_p(400)/C_p(450)$. If SLP is added first, it becomes insignificant when PCO and ORG are added. PCO removes 6% of the variance with a t-value of 2.87, but adding ORG removes an additional 43% of the variance and the t-values become 7.30 and -10.5 for PCO and ORG respectively. PO and P3 also enter the final regression and together remove an additional 6 1/2% of the variance. The t-values are shown in Table XVII. It appears to be the contrast between PO and P3 that is most important. P5 does not enter perhaps because the strong contrast between PCO and ORG is mostly a function of volume which is correlated extremely well with P5 ($r = 0.94$).

The particle size distribution is the single factor that best predicts the spectral characteristics of the beam attenuation. Biological factorw which can reasonably be assumed to relate to the complex index of refraction distribution plays a lesser role perhaps because of an imperfect relationship between the available parameters and the index of refraction. It is difficult to explain why the volume concentration would

TABLE XVII

T-VALUES FOR THE REGRESSION EQUATIONS
PREDICTING SPSE = Cp(400)/Cp(450)

VARIABLES	t-values PCO	ORG	PO	P3	r^2
	2.87				.059
	7.30	-10.50			.491
	7.85	-10.92	2.50		.515
	6.42	-10.63	3.55	-3.46	.550

be a factor unless it is related to errors in calibration or imperfect knowledge of the attenuation spectra for pure seawater. An additional possibility is that the volume concentration is related to the concentration of dissolved organic compounds which may have an effect on the absorption spectra. However, since "yellow matter" as these dissolved organics are collectively called have very steeply sloped spectra towards the shorter wavelengths, there would have to be a negative correlation between VOL and "yellow matter" as VOL was negatively correlated with the spectral parameters discussed above. This may be possible.

Particle Predictions:

Of practical concern is the possibility of predicting particle size distributions from optical spectra. Histograms of the particle parameters PO-P6, VOL for the NASA1 cruise reveal much skewness. Therefore, the natural logarithms of these parameters, LPO-LP6, LVOL, will be used in the subsequent regression analyses as the logarithmic transforms are more normally distributed. The hyperbolic slope, SLP, is not skewed so it is

left unchanged. Both stepwise and backstep routines are used. Generally, the variance is substantially reduced by the first two or three parameters and then a combination of two or three more parameters also produce significant t-values. These combinations are left out unless they reduce the variance by at least 1% per parameter. Lesser reductions are hardly useful and the complex relationships are impossible to interpret physically. The choice between models arrived at by forward and backward stepping is made on the basis of variance removed and the number of parameters involved. Table XVII gives some general information on the particle parameters and the chosen regression.

TABLE XVIII

Standard errors for the particle parameters and the residual error and percent of variance removed by the chosen regression.

Parameter	standard error	residual error	% of variance removed	# of independent variables chosen
LP0	0.73	0.69	10.5	1
LP1	0.55	0.49	23.5	2
LP2	0.57	0.47	30.9	5
LP3	0.59	0.42	49.6	5
LP4	0.79	0.45	67.3	2
LP5	1.35	0.81	64.4	2
LP6	1.68	1.01	64.2	2
LVOL	0.75	0.38	74.9	2
SLP	0.61	0.42	52.8	2

From Table XVIII, it is apparent that the variance of the large particles is much greater than that of the small particles. Therefore, the large particles have a large effect on the attenuation spectra and conversely the spectral parameters remove a large portion of the variance of the concentration of large particles. However, the residual error is

also larger for the large particles. This is not surpising since the low number of large particles counted allows larger relative sampling errors. The regression equations are given in Table XIX.

TABLE XIX

Regression equations for predicting the particle parameters. The standard errors of the regression coefficients are given in parentheses.

LP0 = 8.512 (0.111) + 0.338 (0.062) LCT

LP1 = 4.330 (0.497) + 4.171 (0.667) SPES + 0.564 (0.064) LCT

LP2 = 7.188 (1.349) + 5.629 (2.026) SPM + 8.703 (2.465) SPSE - 53.224 (12.629) SPET - 13.719 (4.696) SPES + 0.501 (0.080) LCT

LP3 = 3.519 (4.012) - 9.090 (2.845) SPE + 7.148 (3.126) SPME + 9.418 (3.191) SPSE - 35.029 (8.420) SPET + 0.476 (0.064) LCT

LP4 = 4.299 (0.327) - 0.971 (0.220) SPE + 0.982 (0.085) LCT

LP5 = 5.969 (0.582) - 3.557 (0.392) SPE + 0.982 (0.085) LCT

LP6 = 4.208 (0.728) - 4.193 (0.490) SPE + 1.257 (0.107) LCT

LVOL = 0.058 (0.272) - 1.420 (0.183) SPE + 0.727 (0.040) LCT

SLP = 1.821 (0.302) + 1.973 (0.204) - 0.290 (0.044) LCT

LCT is used because theoretically the particle concentration should be linearly dependent (assuming other variables constant) on the particulate beam attenuation and thus by transformation the logarithmic particle concentrations should be proportionate to the logarithmic of the attenuation.

The large particles and volume are inversely related to the spectral ratio SPE = $C_p(400)/C_p(650)$ and positively correlated to LCT. Since the hyperbolic slope of the particle size distribution is highly (negatively) correlated to the concentration of large particles and total volume, the same (with reverse signs) hold true for SLP. The situation is much more complex for the small particles since slope and volume depend very little

on them. The complex spectral relationships for the small particles may indicate that pigment absorption spectra for types of phytoplankton may be producing the limited amount of spectra variation from which their concentration can be deduced.

It may be that the relationship between SPE and LCT may provide a universal tool for examining relative particle sizes within any given region, but the absolute values of the coefficients for these regressions are not likely to be constant from region to region or from season to season. The more complex regressions of the small particles are probably useless in other regions and times. At present we have too little data to test the universality of our results.

Conclusions:

It has been demonstrated that both particle size distributions and biological parameters presumably related to the index of refraction of the particles affect the spectral properties of inherent optical parameters. However, the combination of the two effects are nonlinear and thus relationships at one depth, location and time may not hold at another depth, location or time. For this reason, a better approach to this problem would include the following elements.

1) The region of study would be restricted to just the euphotic zone or just the deep or near-bottom zones.
2) The possible optically active constituents of the area would be determined in advance and their optical properties would be determined separately in the laboratory.

3) In situ optical data would be decomposed into the predetermined possible constituents for that depth and region by a minimization technique similar to that employed by Zaneveld et al. (1974).

4) The results would be verified by microscropic chemical and electronic particle sizing techniques on collected samples. If verification is impossible, statistical analyses may suggest modifications to the minimization technique.

5) Areas where the constituents would be very similar would be identified and the technique reaffirmed in a new area.

6) Laboratory studies and known information on the physical and chemical properties of the various elements would be examined to give theoretical relationships between the constituent and its optical signature.

REFERENCES

Draper, N. R. and H. Smith. 1966. Applied regression analysis. John Wiley and Sons. New York. 407 pp.

Gibbs, Ronald J. 1978. Light scattering from particles of different shape. J. Geophys. Res. 83:501-502.

Guthrie, Donald, Carole Avery and Keith Avery. 1974. Statistical interactive programming system (*SIPS) user's reference manual. Technical Report No. 36. Dept. of Statistics. Oregon State Univeristy, Corvallis, Oregon 97331. 111 pp.

Harris, Richard J. 1975. A primer of multivariate statistics. Academic Press, New York. 332 pp.

Jerlov, N. G. 1974. Significant relationships between optical properties of the sea. In: Optical Aspects of Oceanography, Academic Press.

_____. 1976. Marine Optics. Elsevier Sciencitic Publishing Company. Amsterdam, 231 pp.

Kitchen, J. C., D. Menzies, H. Pak and J. R. V. Zaneveld. 1975. Particle size distribution in a region of coastal upwelling analyzed by characteristic vectors. Limnol. Oceanogr. 20: 775-783.

_____, J. Ronald V. Zaneveld and Hasong Pak. 1978. The vertical structure and size distributions of suspended particles off Oregon during the upwelling season. Deep-Sea Res. 25:453-468.

Morel, A. 1973. Diffusion de la lumiere par les eaux de mer: Resultats experimentaux et approche theoretique, AGARD Lecture Series No. 61 on Optics of the Sea.

Mueller, J. L. 1973. The influence of phytoplankton on ocean color spectra. Ph.D. Thesis. Oregon State University. 239 pp.

Shifrin, K. S. and I. N. Salganik. 1973. Light scattering by models of seawater. U.S.S.R. Acad. of Sciences. Leningrad. 217 pp.

Sullivan, S. A. 1963. Experimental study of the absorption in distilled water, artificial seawater, and heavy water in the visible region of the spectrum. J. Opt. Soc. Am., 53: 962-967.

Zaneveld, J. Ronald V., James C. Kitchen, Robert Bartz, David Menzies, Sandy Moore, Richard Spinrad and Hasong Pak. 1978. Optical, hydrographic and chemical observations in the Monterey Bay Area during May and September 1977. Data Report to National Aeronautics and Space Administration contract NAS5-23738. Ref. 78-13. School of Oceanography, Oregon State University. 216 pp.

Zaneveld, J. R. V., D. M. Roach and H. Pak. 1974. The determination of the index of refraction distribution of oceanic particulates. J. Geophys. Res. 79:4091-4095.

APPENDIX

Corrections to the data report, Optical, Hydrographic and Chemical Observations in the Monterey Bay Area during May and September, 1977 by J. Ronald V. Zaneveld et al., 1978.

page 1	First sentence should read, "During May and September of 1977...."
page 91	Second paragraph should end, ".... of total volume can be obtained from the given data."
page 97	Next to last line should read, "10-08 010 ....."
page 106	The following data should be inserted after page 106:

NASA2 SEP 1977

SAMPLE IDENTIFICATION		VOL.	SLOPE	CORR.
15-01	000 METERS	1.515	3.83	.9794
15-01	005	1.714	3.66	.9823
15-01	010	1.268	4.14	.9822
15-01	025	.197	4.27	.9915
15-01	050	.122	4.43	.9946
15-01	100	.121	4.54	.9940
15-02	000	1.151	3.83	.9844
15-02	005	1.504	3.83	.9890
15-02	010	.704	3.82	.9924
15-02	025	.497	3.90	.9891
15-02	050	.162	4.10	.9949
15-02	100	.271	5.26	.9958
15-03	000	.807	3.94	.9890
15-03	005	1.213	3.75	.9925
15-03	010	1.077	3.67	.9911
15-03	025	.455	4.10	.9976
15-03	050	.200	4.47	.9942
15-03	075	.216	4.78	.9899
15-04	000	.304	4.41	.9901
15-04	005	.451	4.15	.9888
15-04	010	.708	4.33	.9840
15-04	025	.172	4.21	.9886
15-04	050	.198	4.92	.9956
15-04	062	.200	5.13	.9879
15-05	000	.250	4.39	.9874
15-05	005	.439	4.03	.9854
15-05	010	.464	4.07	.9895
15-05	015	.559	3.91	.9904
15-05	025	.390	3.86	.9928
15-06	000	.438	4.00	.9950
15-06	005	.436	4.22	.9898
15-06	010	.545	3.99	.9873
15-06	015	.481	4.22	.9936
15-06	020	.430	4.07	.9945
15-06	FILTERED METERS	.083	4.62	.9960
15-07	000	.417	4.05	.9950
15-07	005	.383	4.27	.9904
15-07	010	.548	4.02	.9883
15-07	015	.715	3.99	.9943
15-08	000	.340	4.55	.9835
	050	.387	4.40	.9840
15-08	010	.391	4.66	.9928
15-08	015	.385	4.20	.9811

The following data corrections should be made:

Page	Sample			Parameter	Old Value	New Value
121	04	06	0	B(135, 550)	5302	211
124	09	04	0	B(135, 400)	46	232
125	10	05	5	B(90, 400)	342	732
125	10	09	5	B(135, 400)	1739	227
125	10	09	5	B(135, 450)	1652	256
125	10	09	5	B(135, 500)	1683	301
125	10	09	5	B(135, 550)	1626	297
125	11	01	0	B(90, 400)	500	1071
125	11	01	0	B(90, 450)	490	1014
125	11	02	10	B(135, 450)	85	398
127	12	08	0	B(90, 500)	202	404
129	07	03	5	B(45, 500)	3323	1662
129	07	03	5	B(135, 500)	119	202
129	07	03	5	B(45, 550)	463	1852
129	07	03	5	B(135, 500)	256	187
130	08	05	90	B(45, 550)	194	388
130	08	05	90	B(135, 550)	127	117
130	09	04	5	B(45, 400)	768	1645
130	09	04	5	B(135, 400)	368	324
133	13	03	10	B(90, 500)	87	174
133	13	03	10	B(90, 550)	114	228
133	13	03	15	B(135, 550)	37	331
133	13	03	20	B(135, 550)	48	178
133	Note: repetitions of stations 13-05 and 13-06 are ozoned samples.					
133	13	06	0	B(135, 550)	29	192
134	15	01	10	B(135, 400)	68	265
134	15	01	10	B(135, 500)	541	226
134	15	02	0	B(135, 500)	412	156
134	15	03	5	B(45, 550)	262	2183
134	15	03	5	B(135, 550)	233	137
134	15	03	10	B(45, 550)	284	2367
134	15	03	10	B(135, 550)	266	162
135	15	07	15	B(45, 550)	615	1230
135	15	07	15	B(135, 550)	212	182
135	16	01	15	B(45, 550)	2846	1423
135	16	01	15	B(135, 550)	74	145
165	05	02	000	TR 550	37.2	47.2
165	06	04	005	TR 550	.5	5.0
167	10	01	000	TR 450	4.9	3.8
				TR 500	7.9	5.2
				TR 550	8.0	6.0
				TR 600	6.4	5.4
				TR 650	6.4	4.5
167	10	08	000	Replace data with 13.1, 13.3, 13.5, 13.8, 10.2, 7.7		
170	10	03	060	Sample 10 03 060 13 03 060		
173	06 - 05		1	Replace TR data with 32.1, 35.0, 41.8, 39.9, 34.4, 26.6		
176	08 - 04		25	TR 400	20.2	70.2
181	09 - 03		65	TR 650	69.0	64.0
187	10 - 08		20	TR 650	88.1	58.1
197	12 - 03		10	Replace TR data with 54.9, 61.4, 66.7, 61.6, 55.2, 48.2		
206	14 - 05		10	Replace TR data with 34.9, 38.1, 45.0, 44.6, 33.1, 35.4		